Science of the Total Environment 714 (2020) 136628

Contents lists available at ScienceDirect

Science of the Total Environment

journal homepage: www.elsevier.com/locate/scitotenv

Sorption of oxytetracycline in particulate organic matter in soils and sediments: Roles of pH, ionic strength and temperature

Xinghua Liu [a,d], Haibo Zhang [b,*], Yongming Luo [c,d,**], Rongsheng Zhu [a], Huaizhong Wang [a], Baohua Huang [a]

[a] Institute of Animal Science and Veterinary Medicine Shandong Academy of Agricultural Sciences, Key Laboratory of Livestock Disease Control and Breeding, Jinan, Jinan 250100, China
[b] Key Laboratory of Soil Contamination Bioremediation of Zhejiang Province, School of Environmental and Resource Sciences, Zhejiang A & F University, Hangzhou 311300, China
[c] Institute of Soil Science, Chinese Academy of Sciences, Key Laboratory of Soil Environment and Pollution Remediation, Nanjing 210008, China
[d] Yantai Institute of Coastal Zone Research, Chinese Academy of Sciences, Key Laboratory of Coastal Environmental Processes and Ecological Remediation, Yantai 264003, China

HIGHLIGHTS

- Soil and sediment POMs show distinct properties in component and organic moieties.
- Specific surface area and CEC of the POM have high contributions to OTC sorption.
- Carboxyl group and aliphatic carbon content are correlated with OTC sorption.
- The Ca^{2+} cation showing significant inhibition of the OTC sorption in all POMs

GRAPHICAL ABSTRACT

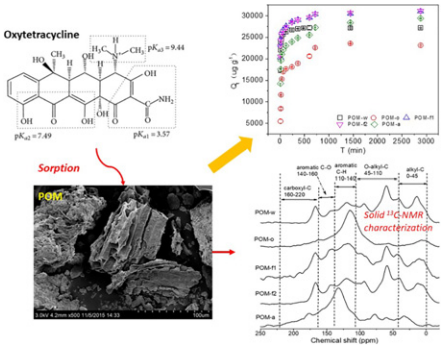

ARTICLE INFO

Article history:
Received 28 October 2019
Received in revised form 24 December 2019
Accepted 8 January 2020
Available online 15 January 2020

Keywords:
Sorption
Oxytetracycline
Soil
Particulate organic matter
Organic functional groups

ABSTRACT

Particulate organic matter (POM) is a fraction of organic matter with dissimilar properties in different soils. POM isolated from soils and sediments (wetland, oil waste field, farmlands and aquaculture pond sediment) was used to study its sorption behavior on the antibiotic oxytetracycline (OTC). Impacts of solution pH, ionic strength and temperature on the OTC sorption were studied. The sorption rates of OTC in POM from wetland (POM-w) and farmland (POM-f1, POM-f2) were rapid during the first 3 h and gradually decreased with reaction time until reaching the equilibrium. Linear sorption occurred from 3 to 12 h in POM from oil waste field land (POM-o) and aquaculture pond sediment (POM-a). The organic carbon normalized partition coefficient (k_{oc}) varied from 215.0 to 4493.6 L kg^{-1}, and it was nearly 10× higher for the POM-w, POM-f1 and POM-f2 than in the POM-o and POM-a. Sorption of OTC by POM exhibited strong pH dependence. Ionic factors affected OTC sorption in POM-f1, POM-f2 and POM-a. The sorption capacity declined >50% in a solution with Ca^{2+} compared to other ions with similar ionic strength. Sorption thermodynamics showed an entropy increasing and endothermic progress during the OTC sorption in POM, implying a spontaneous sorption process. Several mechanisms were involved in OTC sorption in POM, including hydrogen bonding, cation exchange, hydrophobic partitioning and surface complexation.

* Correspondence to: H. Zhang, Zhejiang A & F University, Hangzhou 311300, China.
** Correspondence to: Y. Luo, Institute of Soil Science, Chinese Academy of Sciences, Nanjing 210008, China.
E-mail addresses: hbzhang@zafu.edu.cn (H. Zhang), ymluo@issas.ac.cn (Y. Luo).

https://doi.org/10.1016/j.scitotenv.2020.136628
0048-9697/

1. Introduction

The heavy use of veterinary pharmaceuticals in animal husbandry has increased the amounts of these compounds in the environment. About 77,000 tons of antibiotics are used in animal husbandry each year in China, and yearly antibiotic discharges are estimated to range from 31,000 to 46,000 tons (Zhang et al., 2015b). Metabolism rates range from 40% to ~60% in animals (Wang and Wang, 2015). Relatively small amounts of antibiotics are absorbed during animal metabolism, and the majority is excreted, unmetabolized, via feces and urine (Wang and Wang, 2015). Tetracyclines are the most widely used veterinary antibiotics in the world. They have a broad-spectrum antimicrobial activity against a variety of disease-producing bacteria and are often used in therapy and in the livestock industry (Thiele-Bruhn, 2003). Due to the use of animal manure and sewage sludge as fertilizers in agriculture, tetracyclines can occur in many soil and aquatic environments (Gothwal and Shashidhar, 2015; Kümmerer, 2009). Residues of tetracyclines are frequently found in soil (Zhang et al., 2015a), sediment (Liu et al., 2016), surface water (Zhang et al., 2015b), groundwater (Ma et al., 2015), and wastewater (Rodriguez-Mozaz et al., 2015). Exposure to low-level antibiotics and their transformation products in the environment could be toxic to animals and causes an increase of antibiotic-resistant genes among microorganisms (Sarmah et al., 2006).

Despite their widespread use in veterinary pharmaceuticals and ubiquitous presence in the environment, information on the environmental transport and fate of tetracyclines is limited. Sorption in soils and sediments plays an important role in the environmental behavior and bioavailability of organic contaminants (Wang and Wang, 2015). Tetracyclines have a high adsorption to clay materials, soils, and sediments (Bao et al., 2013; ElSayed and Prasher, 2014; Fernández-Calviño et al., 2015). Several other studies demonstrated that soil/sediment organic matter plays a greater role in the sorption process than soil mineral composition (Guo et al., 2017; Qin et al., 2018; Wang et al., 2018; Zhao et al., 2012). Experiments with humic acid demonstrated that tetracycline sorption in organic matter is primarily driven by cationic exchange/bridging and surface complexation reactions (H-bonding and other polar interactions) between the functionalities (amino, carboxyl, and phenol) of the tetracycline molecules (Aristilde et al., 2010; Figueroa et al., 2004; Kulshrestha et al., 2004; Zhang et al., 2018).

Soil organic matter is a complex, heterogeneous material. In addition to the well-known humic fractions such as humic acid, fulvic acid, and humin, there is considerable particulate organic matter (POM) which consists of light-density, sand complex organic debris with a relatively rapid turnover (Guo et al., 2010). POM is more likely to be free from binding to other soil components such as soil minerals although some POM can be occluded within microaggregates and macroaggregates (Six et al., 2002). POM is a key organic matter fraction that influences soil fertility and can be used as an indicator of soil quality (Besnard et al., 1996). POM accumulates at the soil surface and its interaction with pollutants is important. However, few studies have evaluated the interaction between POM and heavy metals (Guo et al., 2006; Labanowski et al., 2007) and polycyclic aromatic hydrocarbons (PAHs) (Guo et al., 2010; Labanowski et al., 2007). POM interaction with hydrophilic organic contaminants (e.g., antibiotics) remains unknown. The sorption of antibiotics in extracted POM may differ, due to the complicated structures and surface properties, from the sorption of pure humic substances, which were used in previous experiments.

The objective of this work was to characterize and quantify sorption of oxytetracycline (OTC), a widely used tetracycline antibiotic, in five POMs with contrasting properties. The POM properties were characterized by elemental analysis, Fourier transform infrared (FT-IR) spectroscopy and solid-state ^{13}C nuclear magnetic resonance (NMR) to elucidate the relevant mechanisms for sorption of OTC in POM. These results provide a better understanding of POM regulation of antibiotic partitioning in soil-solution systems.

2. Materials and methods

2.1. Materials

OTC was obtained from Dr. Ehrenstorfer GmbH, Germany (99% purity) and used as received. Water used in the study was purified by distillation. Methanol (liquid phase) was purchased from Merck Company (Darmstadt, Germany) with High-Performance Liquid Chromatography (HPLC) grade. Other chemical reagents were all analytical grade and purchased from Sinopharm Chemical Reagent Co., Ltd. (China).

Five soil or sediment samples were collected from the surface (depth, 0–20 cm) of typical different land use zones including wetland, oil waste land, two farmlands (wheat land and corn field) and aquiculture pond sediment in the Yellow River delta, geographically spanning (37°35′N-38°12′N; 118°33′E-119°20′E). The zones were located in northern Shandong province, north China. The pH values of the soils with a soil:water ratio of 1:2.5 (w/v) were 7.6, 8.5, 8.4, 8.8, and 8.5, and the soil organic matter contents were 4.52%, 0.64%, 1.97%, 2.64%, and 0.29% for Soil-w, Soil-o, Soil-f1, Soil-f2 and Soil-a, respectively. These soils were sampled for POM separation to determine their different soil organic matter contents related to their different POM origins and degree of humification. The corresponding POMs were labeled as POM-w, POM-o, POM-f1, POM-f2 and POM-a, respectively. Physical fractionation of the POM was achieved using the method described by Six et al. (1998). Briefly, the soil samples were air dried and passed through 2000 μm, 250 μm and 53 μm nylon sieves sequentially within the purified water to obtain soil fractions in 250–2000 μm, 53–250 μm and < 53 μm. POM in the three soil fractions was separated separately by density extraction using NaI (density, 1.85 g cm^{-3}) and repeated flotation panning in purified water, and finally, oven-dried at 55 °C. There was insufficient 250–2000 μm aggregate to complete the POM separation and less POM separated from <53 μm fraction. Hence, the POM in fraction 53–250 μm was used in the experiments. The fractions of POM represented 0.492%, 0.282%, 0.027%, 0.034% and 0.011% of the bulk soils (w/w) for POM-w, POM-o, POM-f1, POM-f2 and POM-a, respectively.

2.2. Analytical methods

The total organic carbon content of the POM was determined using a C N Elemental Analyzer (Vario Micro, Elementar Analysensysteme GmbH) and the method details were described by (Liu et al., 2019). Infrared spectra were obtained using a Fourier transform infrared (FT-IR) spectrophotometer (FT/IR-4100, JASCO Corporation, Japan) equipped with deuterated triglycine and mercury-cadmium-telluride detectors (Thermo Scientific Nicolet, Madison, WI, USA), a KBr beam splitter (Thermo Scientific Nicolet), and a sample bench dried with dry air. The spectra were obtained by accumulation of 32 scans at a resolution of 4 cm^{-1} in the range of 4000–400 cm^{-1}.

Organic carbon functional groups of the POMs were measured using solid state ^{13}C nuclear magnetic resonance (NMR) spectroscopy (Varian Infinity Plus 400 MHz, VARIAN medical systems, USA). The 0.5 g POMs sample was treated with 10% hydrofluoric acid followed by placed in a sample tube (7 mm diameter) to determine the soil chemical shift composition. The following spectrometer parameters used to acquire the ^{13}C spectra were used: contact time of 2.0 ms; recycle delay time of 1.0 s; spinning speed of 10 kHz and the number of scans ranged from 5000 to 10,000 per sample. Chemical shifts were divided into alkyl-C (0–45 ppm), O-alkyl-C (45–110 ppm), aromatic C—H (110–140 ppm), aromatic C—O (140–160) and carboxyl-C (160–220 ppm) bands (Kögel-Knabner, 1997). The area under the spectrum curve was calculated for the relative content of different functional group classes, which was showed as the proportion of peak area to total spectrum curve area.

The special surface area was measured using a Surface Area and Porosimetry Analyzer (NOVA3200e, Quantachrome Instruments, Florida, USA) with the Brunauer-Emmett-Teller (BET) capacity method

(Van Erp and Martens, 2011). Cation exchange capacity (CEC) was measured by the international standard method (Remusat et al., 2012) and determined using an Inductively Coupled Plasma Optical Emission Spectrometer (ICP-OES). The pH_{pzc} was obtained using pH drift test (Ferro-Garcia et al., 1998). Elemental analysis and scanning image was inspected by reflected light microscopy and scanning electron microscopy in combination with energy dispersive X-ray spectroscopy (SEM-EDX) on the micrometer scale. The SEM-EDX analyses were conducted with a Hitachi S-4800 with a tungsten cathode equipped with a HORIBA EX-350 EDX.

Aqueous OTC concentration was quantified using Waters ACQUITY Ultra Performance Liquid Chromatography (UPLC) -Class with PDA detector. 1.7 μm BEH C_{18} column (2.1 mm × 50 mm; Waters ACQUITY UPLC) was used for quantification of OTC in solution. Samples were isocratic elutions with a mobile phase of 0.126% oxalic acid (80%), acetonitrile (10%) and methanol (10%) flowing at 0.3 mL min^{-1}. The detector wavelength was set at 355 nm, 35 °C column temperature and 2 μL of injection volume. The instrument limit of detection was 0.1 μg L^{-1}.

2.3. Sorption experiments

2.3.1. Isotherms and kinetics

Batch equilibrium sorption experiments were carried out using a batch equilibration (Guideline, 2001). For each replication 0.1000 g POM and 20 mL OTC solution were mixed in a 50 mL polytetrafluoroethylene (PTFE) centrifuge tube, which was then shaken in a thermostat shaker at 200 rpm in darkness. The background solution was 0.01 mol L^{-1} sodium chloride (NaCl) in deionized water with 100 mg L^{-1} sodium azide (NaN_3) as a biocide. Due to low aqueous solubility of the OTC, stock solutions were made in methanol before being added to the background solution. The concentration of methanol in the final solutions was maintained below 0.5% (v/v) to minimize co-solvent effects. Each experiment included blanks, contrasts and three replications. The sorption kinetic study experiments were conducted at 25 °C (298 K, pH 7.0); the initial OTC concentration was set as 150 mg L^{-1} for each POM with the same specification, and the time intervals were set at 5 min, 10 min, 15 min, 30 min, 1 h, 2 h, 4 h, 8 h, 12 h, 24 h and 48 h. After the sorption process, a desorption process was carried out and the time intervals were the same as those used in the sorption process. The sorption isotherm experiments were carried out at 25 °C (298 K, pH 7.0) The concentrations added ranged from 5 to 500 mg L^{-1} (5, 10, 30, 60, 100, 150, 200 and 500 mg L^{-1}), and the equilibrium time was set as 24 h, which was measured in the kinetics experiments. After the 24 h equilibration period, the samples were centrifuged for 5 min at 3000 rpm. The supernatants were passed through 0.22 μm membranes (Millex; Millipore Corp., Billerica, MA) and transferred to 1.5 mL amber vials (Shanghai ANPEL Scientific Instrument Co. Ltd.) for UPLC analysis.

2.3.2. Environmental factors

Environmental factors, including pH, salinity and temperature were examined. In the pH experiment, the initial pH solution values (3.0, 4.0, 6.0, 7.0, 8.0, 9.0, 10.0, 12.0) were adjusted by 0.1 mol L^{-1} hydrochloric acid and 0.1 mol L^{-1} sodium hydroxide to ensure equal sample volume and ion strength after adjusting the initial pH different values. Initial concentration was set as 150 mg L^{-1} with 0.1 mol L^{-1} NaCl used as a background solution. The ionic strength experiment was conducted using different anionic and cationic solutions of the same initial ionic strength. The experiment was initiated with the conductance gradient ranging from 0.00 mS cm^{-1} to 7.90 mS cm^{-1} (0.00, 1.00, 2.70, 4.20, 5.80 and 7.90 mS cm^{-1}) and the concentration of OTC was 150 mg L^{-1}. For the reaction temperature experiment, the sorption isotherm experiments were carried out at 25 °C (298 K), 30 °C (303 K), 35 °C (308 K) and OTC concentrations were the same as in the isotherm experiments.

2.4. Data analysis

The sorption of OTC by heterogeneous sorbents at time t, Q_t (mg kg^{-1}), was calculated by the equation ($Q_t = \frac{V(C_0 - C_t)}{m}$), where C_0 and C_t are the initial and t time concentrations of the OTC (mg L^{-1}) in the solution, respectively. V is the volume of the solution (L), and m is the weight of the POM samples (g). Many compact formulas, such as the pseudo-first model ($\ln(Q_e - Q_t) = \ln Q_e - k_1 t$), pseudo-second model ($\frac{1}{Q_t} = \frac{1}{k_2 Q_e^2} + \frac{1}{Q_e} t$) and intraparticle diffusion model ($Q_t = k_{diff} t^{0.5} + C$) have been used for correlating kinetic data. Isotherm sorption was regressively analyzed using three different sorption models, that is, linear model ($Q_e = K_d C_e$), Langmuir model ($\frac{1}{Q_e} = \frac{1}{Q_e \times Q_{max} \times C_e} + \frac{1}{Q_e}$) and the Freundlich model ($Q_e = K_f C_e^n$). The organic carbon normalized sorption constant, k_{oc}, was calculated based on the organic carbon content, f_{oc} (%), using the equation ($k_{oc} = \frac{k_d}{f_{oc}}$). The sorption thermodynamics parameters were calculated by the following equations (Li et al., 2014). The standard Gibbs free energy change (ΔG^0), standard enthalpy change (ΔH^0), and standard entropy change (ΔS^0) were determined from K_d. (ΔG^0) = $-RT\ln K_0$, $\Delta G^0 = \Delta H^0 - T\Delta S^0$, and $\ln K_d = -\frac{\Delta H^0}{RT} + \frac{\Delta S^0}{R}$, where ΔH^0 and ΔS^0 were obtained

Table 1
Main characteristics of particulate organic matter (POM) separated from different soils.

Parameters	POM (53–250 μm)				
	POM-w	POM-o	POM-f1	POM-f2	POM-a
Soil types	Orthic Halosols	Orthic Halosols	Udic Cambisols	Udic Cambisols	Orthic Halosols
Land types	Saltmarsh	Uncultured land	Wheat field	Corn field	Aquacultural sediment
Special surface area (m^2 g^{-1})	6.41	4.09	7.27	9.59	4.43
Mesoporous surface area (m^2 g^{-1})	3.66	2.01	3.76	5.57	2.7
Microporous surface area (m^2 g^{-1})	0.86	0.66	1.28	0.31	0.13
CEC (cmol kg^{-1})	19.33	19.27	19.33	19.32	19.28
Total organic carbon (g kg^{-1})	172	325	189	169	210.3
Alky-C (%)	22.8	13.0	11.9	17.3	15.1
O-alky-C (%)	38.9	0	37.2	37.2	7.2
Aromatic C—H (%)	17.1	72.2	28.9	22.2	64.5
Aromatic C—O (%)	8.7	11.6	10.9	9.0	6.0
Carboxyl-C (%)	12.5	3.3	11.2	14.3	7.2
pH_{pzc}	5.90	7.29	7.75	7.69	NA
CaO(%)	5.59	10.97	7.46	7.3	12.49
Al_2O_3(%)	19.47	14.95	19.47	20.45	17.4

NA: data not available.

from the slope and intercept of the linear plot of $\ln K_0$ against 1/T. Model fitting and drawing were conducted by Origin 9.0 software. Principal component analysis (PCA) was performed using SPSS 16.0 for windows. All the detected antibiotics values were included in the analysis. The principal components were considered if their Eigenvalues were >1. The Varimax with orthogonal rotation method was selected for rotation in the PCA. The principal component scores were plotted to show the relationship between K_d and the surface properties of the POMs.

3. Results

3.1. Characterization of POM

The characteristics of the isolated POM are presented in Table 1. Special surface areas of POM separated from different land uses were different and were in the following order (high to low): POM-f2, POM-f1 > POM-w > POM-o, POM-a. Most of the special surface areas of the POM were mesoporous surface areas and fewer than 18% were microporous surface areas. The cation exchange capacities (CEC) of POM from different land use soil/sediments were not significantly different. The organic carbon content of farmland POM (POM-f1, POM-f2) was similar to POM-w, and lower than POM-a and POM-o. The solid-state ^{13}C NMR spectra of different POMs (Fig. S1 in Supplementary) demonstrated different chemical shifts, which reflect different types of organic carbon such as aliphatic carbon, aromatic carbon and carboxyl carbon. Their integration results are presented in Table 1. Higher aromatic carbon content and lower aliphatic carbon content suggest a greater humification (Tfaily et al., 2014). The humification degrees of the POM were in the following order: farmland POM (POM-f1, POM-f2) > POM-w. Nevertheless, the difference of aromatic carbon and aliphatic carbon contents for POM-a and POM-o may mainly be caused by different types of human activities and marine organic carbon sources (Liu et al., 2019). The calcium oxide contents of POM-o and POM-a were higher than those of the other three POMs while their aluminum oxide contents were the lowest. This demonstrated that POM from different land uses had different inorganic compositions (Zhou, 1983).

3.2. Sorption kinetics and isotherms

3.2.1. Sorption kinetics

The sorption kinetics process of OTC on different POMs is presented in Fig. 2. The sorption rate on POM-w and farmland POM (POM-f1, POM-f2) was rapid during the first 3 h and gradually decreased with increasing contact time until equilibrium at 24 h. There was an analogous linear sorption progress from 3 to 12 h, and then the sorption rate gradually decreased until equilibrium, which was also at 24 h for the POM-o and POM-a. At the beginning of the sorption progress, there were sufficient sorption sites on the surface of POM samples (Zhao et al., 2012). The initial concentration of OTC provided the necessary driving force to overcome the resistances of mass transfer on the surface between the OTC solution phase and the POM phase (Gu and Karthikeyan, 2008). With increasing contact time, sorption sites on the POM surface were close to saturation that reduced the rate of sorption transfer from the liquid surface into voids of POM. Due to the increase of the resistance function, the rate of sorption gradually decreased until equilibrium was attained (Watling, 1988). This kinetics process indicated the differences of sorption mechanisms among the POM from different land use areas. Three widely used kinetic models, which were pseudo-first-order, pseudo-second-order kinetic and intraparticle diffusion models were used to interpret the kinetics results. The kinetic parameters and the determination correlation coefficient R^2 are presented in Table 2. The R^2 values obtained by the pseudo-first-order kinetic equation were higher than 0.99, and the calculated Q_e values were close to, and in good agreement with, the experimental results. This indicated that the pseudo-first-order kinetic model fits better than the pseudo-second-order kinetic model. The intraparticle diffusion model was also

Table 2
The fitting parameters of Pseudo-first-order, pseudo-second-order and intra-particle models for OTC sorption in the POM.

POM	Pesudo-first-order fitting				Pesudo-second-order fitting			Intra-particle diffusion model fitting								
	$Q_{e,exp}$ (mg kg^{-1})	$k_1 \times 10^{-3}$ (h^{-1})	$Q_{e,cal}$ (mg kg^{-1})	R^2	$k_2 \times 10^{-4}$(kg (mg h)$^{-1}$)	$Q_{e,cal}$ (mg kg^{-1})	R^2	k_{i1} (mg kg^{-1} min$^{-0.5}$)	C_1 (mg kg^{-1})	R^2	k_{i2} (mg kg^{-1} min$^{-0.5}$)	C_2 (mg kg^{-1})	R^2	k_{i3} (mg kg^{-1} min$^{-0.5}$)	C_3 (mg kg^{-1})	R^2
POM-w	27,168.0	22.4	27,174.6	0.999	0.39	27,193.6	0.982	2194.64	13,983.89	0.681	111.04	24,970.84	0.951	0.38	27,173.11	0.454
POM-o	23,584.5	2.78	26,133.7	0.999	0.061	22,197.9	0.896	3048.48	−1050.53	0.973	162.14	15,776.36	0.964	65.35	20,155.34	0.158
POM-f1	30,499.6	8.90	30,736.5	0.999	0.38	29,451.4	0.893	1699.68	17,335.17	0.855	214.92	25,137.56	0.976	39.44	28,975.13	0.689
POM-f2	30,704.6	8.50	30,908.3	0.999	0.37	29,390.6	0.853	1552.55	17,621.27	0.892	253.36	24,432.94	0.973	41.79	29,010.97	0.670
POM-a	28,416.0	4.06	29,278.6	0.999	0.19	26,185.8	0.835	2046.14	10,583.55	0.838	242.00	20,296.33	0.992	113.78	23,602.79	0.742

Table 3
The isotherm parameters for OTC sorption in the POM.

POM	Linear fitting			Langmuir fitting			Freundlich fitting		
	k_d(L kg^{-1})	k_{oc}(L kg^{-1})	R^2	Q_{max}(mg kg^{-1})	k_1	R^2	k_f((mg kg^{-1}) (mg L^{-1})$^{1/n}$)	1/n	R^2
POM-w	772.9 (57.0)	4493.6	0.97	96,720.2 (14,684.4)	0.019	0.99	209,349.6(46,708.00)	0.772(0.07)	0.99
POM-o	69.9 (9.7)	215.0	0.91	14,690.0 (2537.4)	0.11	0.99	96,967.5(37,481.21)	0.506(0.05)	0.98
POM-f1	673.9 (65.4)	3565.7	0.96	35,854.1 (7756.1)	0.13	0.99	110,724.9(25,042.30)	1.00(0.14)	0.94
POM-f2	666.7 (66.3)	3945.5	0.95	28,708.1 (7939.2)	0.19	0.99	110,204.5(23,566.48)	1.00(0.13)	0.95
POM-a	84.7 (26.3)	403.2	0.70	31,385.7 (12386)	0.06	0.91	45,370.04(4778.53)	0.851(0.09)	0.98

Note: standard errors are indicated in brackets.

used to investigate the kinetic sorption and the results are presented in Fig. S3 in Supplementary and Table 2. Fig. S3 in Supplementary showed that the experimental data points had three linear sections, indicating that the sorption of OTC by POM was related to three consecutive steps. The consistent values are shown in Table 2. The R^2 values of the second line were all higher than 0.95 and the intercepts (C_1 values) were all different from zero indicating that the first line did not pass through the origin. These data suggest that intraparticle diffusion was not the sole rate controlling step in the first steps of sorption and that other processes may influence the sorption rate (Liu et al., 2012). Film-diffusion control may have also occurred in the early stage of the OTC sorption process and the actual sorption process may contain surface sorption and intraparticle diffusion before reaching the equilibrium stage.

3.2.2. Sorption isotherms

The sorption isotherms described by the Linear equation, Langmuir equation and Freundlich equation are presented in Fig. 3. The correlation coefficients and the organic carbon normalized sorption constant k_{oc} are shown in Table 3. The k_d values of the linear sorption isotherm ranged from 69.89 to 772.90 L kg^{-1} and the R^2 ranged from 0.700 to 0.973 for the POM from different land types. The R^2 of POM-a (0.70) was the lowest, while the other R^2 values were all higher than 0.90. This indicated that the sorption isotherm of POM-a was not a linear process. The k_d values on POM were less than values previously reported for soil organic matter. For example, the k_d value for tetracycline was 8400 L kg^{-1} on activated sludge (Kim et al., 2005), and 1140–1620 L kg^{-1} on peat (Sithole and Guy, 1987). This might be due to the complex interaction effect of POM's mineral part shown in Fig. 1. The fractionation and conformational changes in POM substances on sorption to minerals could reduce their reactivity toward OTC since, mineral-bound humic substances could undergo physiochemical and conformational changes (Wang and Xing, 2005).

The Langmuir model suggests that uptake occurs on a homogeneous surface by monolayer sorption and it assumes uniform energies of the sorption onto the surface of the POM. The Freundlich equation parameters (k_f and $1/n$) represent sorption affinity and isotherm nonlinearity, respectively. Table 3 shows that the saturate sorption amount of OTC on the POM varied from 14,690 to 96,720. 22 mg kg^{-1} and that on POM-w was greatest (96,720.22 mg kg^{-1}). The k_l values varied from 0.019 to 0.19 and the POM-w value was the lowest (0.019). The $1/n$ of POM-w was 0.772. Weber and Young (1997) suggested that the $1/n$ value could be used as an index of site energy distribution. Both of the models suggest that the POM-w sorption isotherm was affected by more than one mechanism. The $1/n$ values of POM-o ($1/n = 0.506$) and POM-a ($1/n = 0.851$) were both lower than one. The k_l values were similar and lower than the values of POM-f1 and POM-f2, suggesting that the sorption isotherms of POM-a and POM-o were different. The $1/n$ values equaled one for POM-f1 and POM-f2, demonstrating that the sorption processes of POM-f1 and POM-f2 were linear (Weber and Young, 1997). Linear sorption indicated that partitioning was the dominant mechanism for OTC sorption on POM-f1 and POM-f2, due to its

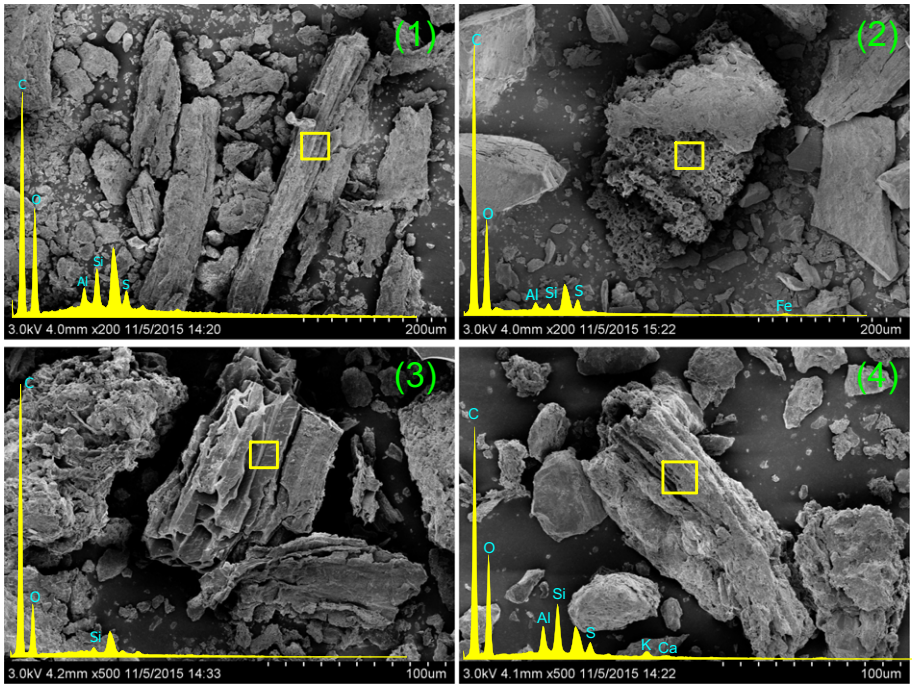

Fig. 1. SEM-EDX images of POM from the differnet soils, which show the comprising of organic and inorganic components in the POM, (1) POM-w, (2) POM-f1, (3) POM-o, (4) POM-a.

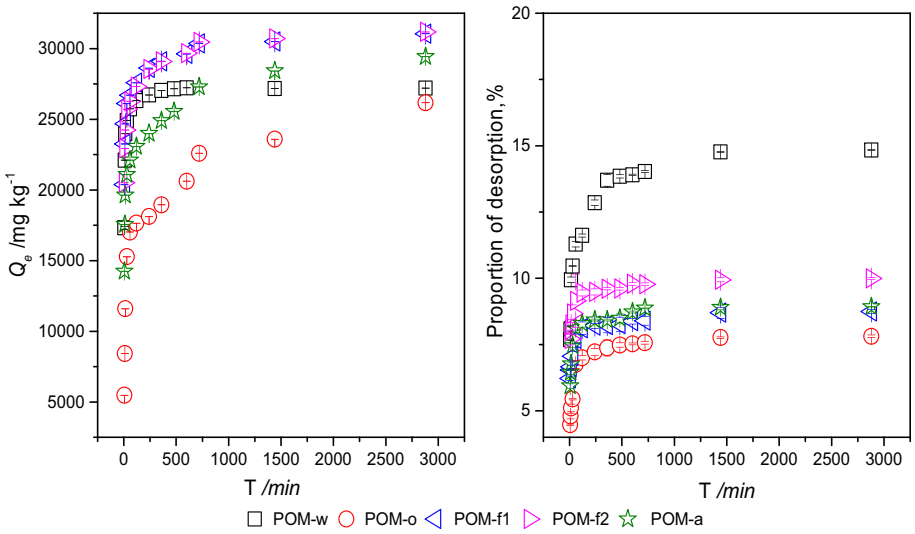

Fig. 2. Sorption kinetics (1) and desorption kinetics (2) of oxytetracycline in the different POMs. (Q_e dentoes the quantity of OTC sorption in the POMs at equibrium. T denotes reaction time).

higher hydrophobicity and lager molecular volumes that resulted in sorption mainly via solid-phase dissolution (Gu et al., 2007).

The organic carbon normalized sorption capacity (k_{oc}) can be an indicator of POM sorption affinity for OTC. In the present study, the k_{oc} value increased with increasing hydrophobicity of the sorbates, which was consistent with previous results (Labanowski et al., 2007). For a given sorbate, the k_{oc} values of POM-w and POM-f1, POM-f2 were nearly 10× higher than the values of POM-o and POM-a. This observation together with the lower values of 1/n indicated that POM-o and POM-a less powerful partition medium was probably due to their lowest aliphatic carbon level and highest aromatic carbon level. Suan and Dmitrenko (1994) reported that k_{oc} values were positively correlated with the level of aliphatic carbon and not correlated with the level of aromatic carbon. The similar k_{oc} values for POM-w and POM-f are mainly due to their similar composition and configuration (Wang and Xing, 2005).

3.3. Effect of environmental factors

3.3.1. Effect of pH

OTC is an amphoteric molecule with multiple groups, such as phenol, amino, and alcohol, that are charged and/or capable of electronic coupling (Chang et al., 2009; Pils and Laird, 2007; Sassman and Lee, 2005). Solution pH values play an important role in OTC exhibiting different ionic forms. Generally, OTC has four different species at various pH values, such as a positive form, a neutral form, one negative valence and two negative valences (Sassman and Lee, 2005). These are shown in Fig. 4(2). The net negative charge ion (+−) is present at pH ≈ 5.5. At pH 7.0, OTC has about 67% neutral zwitterions (ionization is +-0) and 33% zwitterions with a net negative charge (ionization is +−). The two negative valences are present up to pH > 7. At pH 9.0, there is about 29% one negative valence and 71% two negative valences (Sassman and Lee, 2005). The pH effect was investigated by adjusting

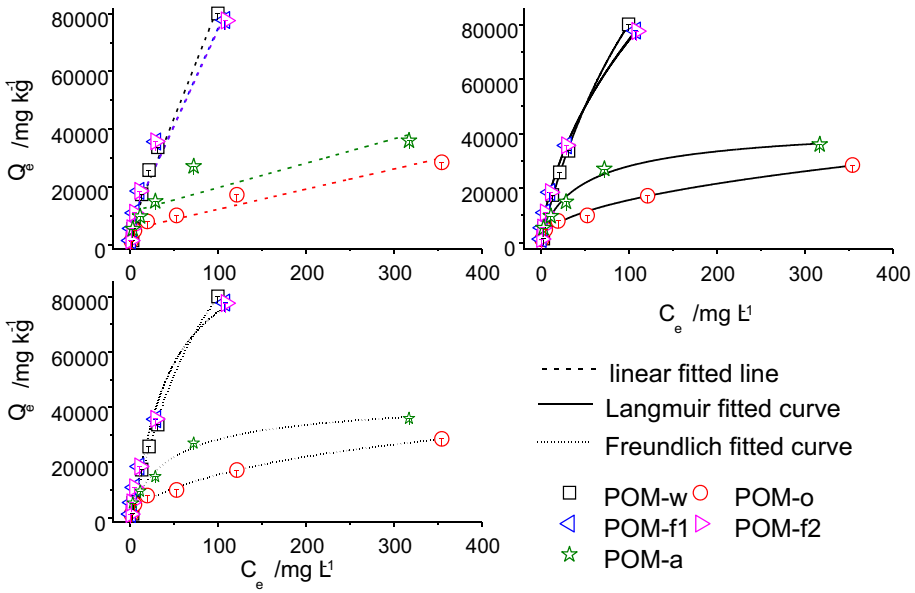

Fig. 3. Sorption isotherms for the oxytetracycline in the different POMs. (Q_e and C_e dentoes the quantity of OTC sorption in the POMs and OTC concentaiton in the supernate at equibrium, respectively).

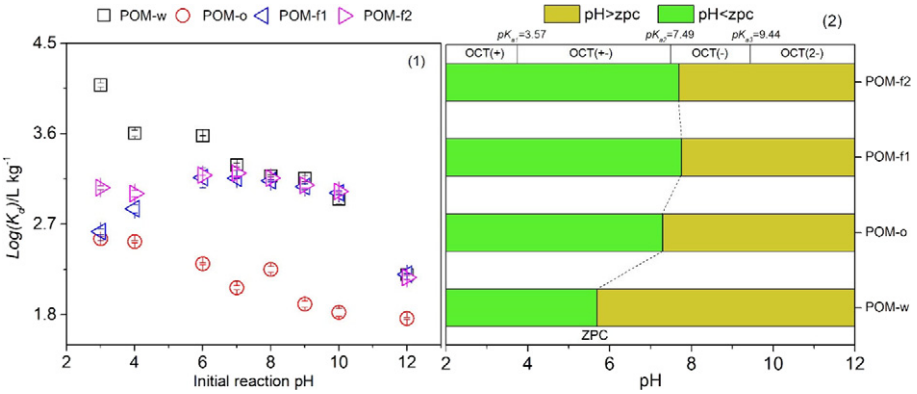

Fig. 4. Effect of solution pH on the oxytetracycline sorption in the different POMs(1), the OTC speciations and the surface charge of the POMs under the different pH condition (2) (K_d is the partition coefficient of OTC between the POM and solution which was calculated using linear model for isotherm sorption).

the pH of initiating sorption solution from 3 to 12. Sorption of OTC to POM exhibited a strong pH dependence and the sorption isotherms of OTC on POM in different pH values are shown in Fig. 4(1). The OTC sorption process of different original POM showed different variation tendencies according the range of pH variation. At a pH < pk_{a1}, the carboxylic groups of POMs are protonated, and OTC is dominated by cations. Higher log(k_d) of POM-w and POM-f2 than the other two POMs is mainly caused by carboxylic groups in the organic matter, probably through a cation exchange mechanism (Gu and Karthikeyan, 2008). With pH in the range of 4–6, OTC is dominated by zwitterions and sorption of OTC on the POM is mainly through H-bonding interactions for POM-w and POM-f1, POM-f2. Sorption of OTC in POM-f1, POM-f2 was caused by hydrophobic effects. When pH > pk_{a2}, electrostatic repulsion dominated the sorption between OTC and all the POMs since both the sorbate (OTC) and the sorbent (POMs, pH_{ZPC} were higher than pk_{a2}) become progressively negatively charged with increasing pH (Gu and

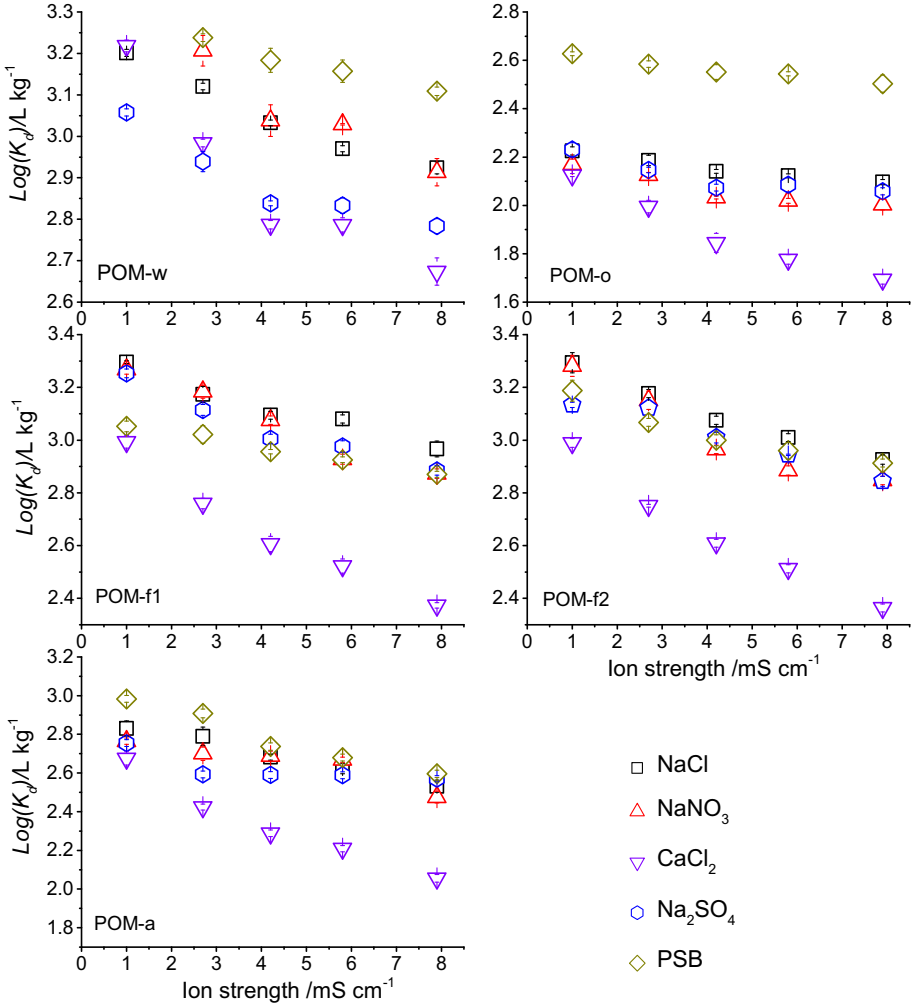

Fig. 5. Effect of ions types and their ionic strength on the oxytetracycline sorption in the different POMs (1) POM-w, (2) POM-f1, (3) POM-f2, (4) POM-o, (5) POM-a (K_d is the partition coefficient of OTC between the POM and solution which was calculated using linear model for isotherm sorption).

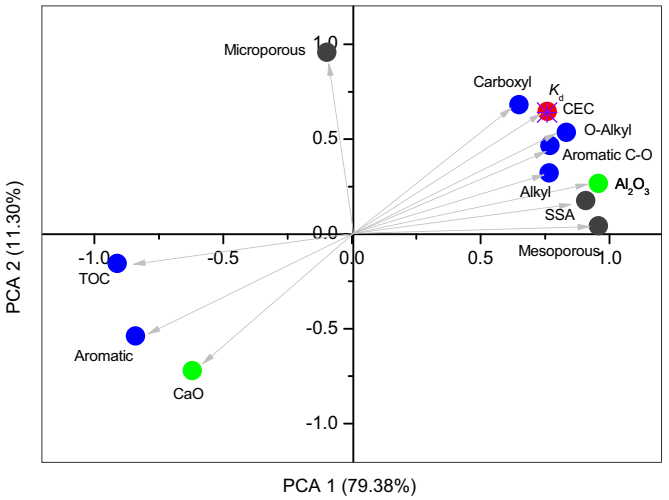

Fig. 6. Principal component analysis (PCA) plots showing correlations between the K_d values and surface properties of the POMs (K_d is the partition coefficient of OTC between the POM and solution which was calculated using linear model for isotherm sorption, CEC denotes cation exchange capacity, SSA denotes specific surface area, TOC denotes total organic carbon).

Karthikeyan, 2008). When pH ranged from 4 to 12, $log(k_d)$ values of POM-o decreased and this was mainly caused by electrostatic interaction.

3.3.2. Effect of ionic strength

Coexisting ions play an important role during OTC sorption in POM. Sorption of OTC in POM is mainly affected through ionic strength and ionic types. The $log(k_d)$ values of OTC sorption in POM with different ionic strength are shown in Fig. 5. A strong dependence occurred for OTC sorption to POM-f1, POM-f2 and POM-a, but the sorption extent decreased by >50% with Ca^{2+} in the background electrolyte concentration than with other ions at the same ionic strength. Cation exchange was proposed as the dominant sorption mechanism for OTC interaction with POM (Gu et al., 2007). SO_4^{2-} slightly inhibited OTC sorption in POM-w mainly controlled by the cation sorption surface and competition by H-bonding. SPB had less inhibition in POM-w, POM-a and POM-o. Solution pH_{PSB} equals to 7, which mainly controlled the sorption process.

3.3.3. Effect of reaction temperature

OTC sorption capacity increased with increasing temperature, indicating that the sorption process was endothermic (Table 4). The negative values of ΔG^0 suggested the feasibility of the sorption process and the positive values of ΔH^0 and ΔS^0 showed that the sorption process was endothermic in nature and had an increase in randomness at the solid/liquid interface during the sorption process, respectively.

4. Discussion

The results demonstrated that physical adsorption occurred between OTC and the surface of the POM samples (Watling, 1988). The maximum OTC absorption capacity of POM from both wetland and farmland is consistent with the larger special surface area of these POMs compared to the other POMs. The slow penetration of OTC by diffusion onto the microporous surface of the interlayers of POM after an initially rapid adsorption onto the external surface and the mesoporous surface has been observed previously (Chang et al., 2009). In this study, the OTC sorption dynamics in the POM-a and POM-o showed an analogous linear sorption process due to the relatively small special surface area, especially the small external surface area and mesoporous surface. OTC sorption in POM-o and POM-a was relatively low (Table 2). Due to the micropore-filling effect (Kögel-Knabner et al., 2008; Mayer, 1994), the large-sized OTC molecule has a low sorption efficiency in the micropores of POM at low solute concentrations because the high-energy small pores are preferentially occupied by small-sized sorbates. Previous studies showed that the reduced adsorption of large-sized tetracycline molecules on black carbon is probably due to the size-exclusion effect (Remusat et al., 2012). The size-exclusion effect was proposed earlier as the mechanism for the impeded adsorption of bulky adsorbate (OTC) molecules on highly microporous carbonaceous adsorbents. This indicated that the main sorption sites of OTC were the inter pores existing in organic matter formation or mineral construction on the analogous sorption process (Aristilde et al., 2010).

In addition to the physical conformation and accessibility, the chemical composition of POM also influences OTC sorption characteristics (Smernik and Kookana, 2015). The PCA results indicated that several surface properties (e.g. carbon functional groups, CEC, SSA) may affect the sorption affinity between OTC and POMs (Fig. 6). POM exists in the form of mineral-organic complexes. The organic matter of POM is the main active component that effects the sorption of OTC. The organic part is derived from the decomposition of plant, animal, microbial biomolecules and constitutes a major sorbent phase for organic contaminants (Ling et al., 2016). The results of FR-IT (Fig. S2 in Supplementary) and ^{13}C NMR (Fig. S1 in Supplementary and Table 1), show that organic matter contains large numbers of functional groups of carboxyl carbon, aliphatic carbon and aromatic carbon. All of these different carbon types have different capacities for bonding to charged OTC ions (Six et al., 1999). However, the high sorption affinity of OTC results from its strong complexation ability due to its polar functional groups (phenol, alcohol, amine, and ketone) (Fig. 6). This process involved organic functional group substitutions between POM and OTC or the interaction of sorption of mineral interlayers (Feng et al., 2013; Kulshrestha et al., 2004; Oehler et al., 2010; Vogel et al., 2014). Previous research verified that dissolved organic matter (DOM) in soil significantly affects the sorption and mobility of organic chemicals (Kulshrestha et al., 2004; Sutton and Sposito, 2005). In this study, k_{oc} values of POM from wetland and farmland were significantly greater than other two POM (Table 3), and k_{oc} values exhibited significant positive correlations with the relative content of POM aliphatic carbon ($R^2 = 0.973$) and negative correlations with relative content of POM aromaticity ($R^2 = 0.993$). These results were consistent with results of other studies (Suan and Dmitrenko, 1994). This indicated that POM-w and POM-f1, f2, had strong sorption capacity, mainly due to their high relative content of aliphatic carbon.

The sorption mechanism differences between POM-w and POM-f1, f2 are due to the relative O-alkyl carbon content. Many other studies have reported that k_{oc} values of hydrophobic organic contaminant were negative with the O-alkyl carbon relative content (Mitchell and Simpson, 2012; Smernik and Kookana, 2015). Regarding the pH effect on sorption processes, the $\log(k_d)$ of POM-w and POM-f1, f2 was nearly constant from pH 6 to 10 indicating that the lipophilic interactions of aliphatic carbon were the main influencing factors. The $log(k_d)$ of POM-a decreased as pH increased from pH 4, indicating that lipophilic interaction was the main sorption mechanism (Pils and Laird, 2007; Sassman and Lee, 2005; Xu and Li, 2010). Both POM-a and POM-o have high aromatic carbon relative content, but the maximum adsorbing capacity of POM-a was much higher than POM-o. This was due to the high relative calcium oxide and aluminum oxide content of POM from the

Table 4
Thermodynamic parameters for OTC sorption in the POM.

POM	ΔG^0(kJ mol^{-1})			H^0(kJ mol^{-1})	ΔS^0(kJ mol^{-1})	R^2
	298 K	303 K	308 K			
POM-w	−14.55	−14.87	−15.51	13.81	0.095	0.700
POM-o	−8.60	−9.60	−10.23	40.09	0.16	0.948
POM-f1	−14.22	−14.75	−15.06	10.97	0.085	0.756
POM-f2	−14.19	−14.69	−15.13	13.89	0.094	0.984

aquaculture pond sediment (Tolls, 2001). In this situation, exchangeable base cations can enhance OTC sorption by interaction of the hydroxylate group or dihydroxy moiety with surface-associated cations (Le Bris, 1996; Loke et al., 2002). This OTC sorption process was competed by solution ions (Fig. 5). This result was not consistent with a previously described mechanism of soil ionic binding of OTC to divalent metal cations, such as Ca^{2+} (Loke et al., 2002). The maximum adsorbing capacity of POM-w was nearly 3× that of POM-f1, f2 and the high relative content of carboxyl was another influencing factor. A previous DOM study verified that TCs sorption on DOM was attributable to ionic interactions and hydrogen bonding via many kinds of reactive functional groups such as carboxyl, hydroxyl and carbonyl (Sedghi et al., 2015).

5. Conclusions

The sorption of OTC to different POMs had variable characteristics due to the various properties of the POMs. POMs with a high special surface area and CEC content showed a higher sorption capacity for OTC owing to the abundant surface sorption sites and ion exchangeable sites. Aliphatic carbon and aromatic carbon on the POM surface had a different effect on OTC sorption. The POM had a high affinity for OTC when it contained a high proportion of aliphatic carbon but a low sorption capacity when it contained a high proportion of aromatic carbon. The carbonyl group on the POM surface enhanced OTC sorption by formation of a hydroxylated group with surface-associated cations. Sorption of OTC by POM was a spontaneously endothermic reaction with entropy increasing in nature. Sorption of OTC in the POM appears to be regulated by several mechanisms, including cation exchange, hydrogen bonding and surface complexation.

CRediT authorship contribution statement

Xinghua Liu: Investigation, Writing - original draft.**Haibo Zhang:** Supervision, Investigation.**Yongming Luo:** Supervision, Resources. **Rongsheng Zhu:** Formal analysis.**Huaizhong Wang:** Software.**Baohua Huang:** Writing - review & editing.

Declaration of competing interest

The authors declare that they have no known competing financial interests or personal relationships that could have appeared to influence the work reported in this paper.

Acknowledgements

The authors are grateful for financial support from the National Natural Science Foundation of China (No. 41371313, 41771351), Shandong Key Laboratory of Coastal Environmental Processes, YICCAS (No. 2019SDHADKFJJ09), Innovation Project of Shandong Academy of Agricultural Sciences (No. CXGC2018E10), Zhejiang Provincial Natural Science Foundation of China (No. LZ19D010001) and the Zhejiang Agriculture and Forestry University Research Fund (No. 2017FR021).

Appendix A. Supplementary data

Supplementary data to this article can be found online at https://doi.org/10.1016/j.scitotenv.2020.136628.

References

Aristilde, L., Marichal, C., Miehe-Brendle, J., Lanson, B., Charlet, L., 2010. Interactions of oxytetracycline with a smectite clay: a spectroscopic study with molecular simulations. Environmental science & technology 44 (20), 7839–7845.

Bao, Y., Wan, Y., Zhou, Q., Li, W., Liu, Y., 2013. Competitive adsorption and desorption of oxytetracycline and cadmium with different input loadings on cinnamon soil. J. Soils Sediments 13 (2), 364–374.

Besnard, E., Chenu, C., Balesdent, J., Puget, P., Arrouays, D., 1996. Fate of particulate organic matter in soil aggregates during cultivation. Eur. J. Soil Sci. 47 (4), 495–503.

Chang, P., Jean, J., Jiang, W., Li, Z., 2009. Mechanism of tetracycline sorption on rectorite. Colloids Surf. A Physicochem. Eng. Asp. 339 (1), 94–99.

ElSayed, E.M., Prasher, S.O., 2014. Sorption/desorption behavior of oxytetracycline and sulfachloropyridazine in the soil water surfactant system. Environ. Sci. Pollut. Res. 21 (5), 3339–3350.

Feng, W., Plante, A.F., Six, J., 2013. Improving estimates of maximal organic carbon stabilization by fine soil particles. Biogeochemistry 112 (1), 81–93.

Fernández-Calviño, D., Bermúdez-Couso, A., Arias-Estévez, M., Nóvoa-Muñoz, J.C., Fernández-Sanjurjo, M.J., Álvarez-Rodríguez, E., Núñez-Delgado, A., 2015. Competitive adsorption/desorption of tetracycline, oxytetracycline and chlortetracycline on two acid soils: stirred flow chamber experiments. Chemosphere 134, 361–366.

Ferro-Garcia, M., Rivera-Utrilla, J., Bautista-Toledo, I., Moreno-Castilla, C., 1998. Adsorption of humic substances on activated carbon from aqueous solutions and their effect on the removal of Cr (III) ions. Langmuir 14 (7), 1880–1886.

Figueroa, R.A., Leonard, A., MacKay, A.A., 2004. Modeling tetracycline antibiotic sorption to clays. Environmental science & technology 38 (2), 476–483.

Gothwal, R., Shashidhar, T., 2015. Antibiotic pollution in the environment: a review. CLEAN–Soil, Air, Water 43 (4), 479–489.

Gu, C., Karthikeyan, K., 2008. Sorption of the antibiotic tetracycline to humic-mineral complexes. J. Environ. Qual. 37 (2), 704–711.

Gu, C., Karthikeyan, K.G., Sibley, S.D., Pedersen, J.A., 2007. Complexation of the antibiotic tetracycline with humic acid. Chemosphere 66 (8), 1494–1501.

Guideline, P.-B.T, 2001. OECD Guideline for the Testing of Chemicals. The Hershberger 601.

Guo, X., Zhang, S., Shan, X., Luo, L., Pei, Z., Zhu, Y., Liu, T., Xie, Y., Gault, A., 2006. Characterization of Pb, Cu, and Cd adsorption on particulate organic matter in soil. Environ. Toxicol. Chem. 25 (9), 2366–2373.

Guo, X., Luo, L., Ma, Y., Zhang, S., 2010. Sorption of polycyclic aromatic hydrocarbons on particulate organic matters. J. Hazard. Mater. 173 (1), 130–136.

Guo, X., Shen, X., Zhang, M., Zhang, H., Chen, W., Wang, H., Koelmans, A.A., Cornelissen, G., Tao, S., Wang, X., 2017. Sorption mechanisms of sulfamethazine to soil humin and its subfractions after sequential treatments. Environ. Pollut. 221, 266–275.

Kim, S., Eichhorn, P., Jensen, J.N., Weber, A.S., Aga, D.S., 2005. Removal of antibiotics in wastewater: effect of hydraulic and solid retention times on the fate of tetracycline in the activated sludge process. Environmental Science & Technology 39 (15), 5816–5823.

Kögel-Knabner, I., 1997. 13C and 15N NMR spectroscopy as a tool in soil organic matter studies. Geoderma 80 (3), 243–270.

Kögel-Knabner, I., Guggenberger, G., Kleber, M., Kandeler, E., Kalbitz, K., Scheu, S., Eusterhues, K., Leinweber, P., 2008. Organo-mineral associations in temperate soils: integrating biology, mineralogy, and organic matter chemistry. J. Plant Nutr. Soil Sci. 171 (1), 61–82.

Kulshrestha, P., Giese, R.F., Aga, D.S., 2004. Investigating the molecular interactions of oxytetracycline in clay and organic matter: insights on factors affecting its mobility in soil. Environmental Science & Technology 38 (15), 4097–4105.

Kümmerer, K., 2009. Antibiotics in the aquatic environment – a review – part I. Chemosphere 75 (4), 417–434.

Labanowski, J., Sebastia, J., Foy, E., Jongmans, T., Lamy, I., van Oort, F., 2007. Fate of metal-associated POM in a soil under arable land use contaminated by metallurgical fallout in northern France. Environ. Pollut. 149 (1), 59–69.

Le Bris, H., 1996. Sorption of oxolinic acid and oxytetracycline to marine sediments. Chemosphere 33 (5), 801–815.

Li, H., Zhang, D., Han, X., Xing, B., 2014. Adsorption of antibiotic ciprofloxacin on carbon nanotubes: pH dependence and thermodynamics. Chemosphere 95, 150–155.

Ling, C., Li, X., Zhang, Z., Liu, F., Deng, Y., Zhang, X., Li, A., He, L., Xing, B., 2016. High adsorption of sulfamethoxazole by an amine-modified polystyrene–divinylbenzene resin and its mechanistic insight. Environmental Science & Technology 50 (18), 10015–10023.

Liu, L., Wan, Y., Y., X., 2012. The removal of dye from aqueous solution using alginate-halloysite nanotube beads. Chem. Eng. J. 187.

Liu, X., Zhang, H., Li, L., Fu, C., Tu, C., Huang, Y., Wu, L., Tang, J., Luo, Y., Christie, P., 2016. Levels, distributions and sources of veterinary antibiotics in the sediments of the Bohai Sea in China and surrounding estuaries. Mar. Pollut. Bull. 109 (1), 597–602.

Liu, X., Zhang, H., Li, Y., 2019. Variation of Organic Matter in Soil Aggregates with the Succession of Tidal Flatland from Barren Land-Saltmarsh-Upland in the Yellow River Delta. p. 56 (2).

Loke, M.-L., Tjørnelund, J., Halling-Sørensen, B., 2002. Determination of the distribution coefficient (logK d) of oxytetracycline, tylosin A, olaquindox and metronidazole in manure. Chemosphere 48 (3), 351–361.

Ma, Y., Li, M., Wu, M., Li, Z., Liu, X., 2015. Occurrences and regional distributions of 20 antibiotics in water bodies during groundwater recharge. Sci. Total Environ. 518–519, 498–506.

Mayer, L.M., 1994. Surface area control of organic carbon accumulation in continental shelf sediments. Geochim. Cosmochim. Acta 58 (4), 1271–1284.

Mitchell, P.J., Simpson, M.J., 2012. High affinity sorption domains in soil are blocked by polar soil organic matter components. Environmental science & technology 47 (1), 412–419.

Oehler, D.Z., Robert, F., Walter, M.R., Sugitani, K., Meibom, A., Mostefaoui, S., Gibson, E.K., 2010. Diversity in the Archean biosphere: new insights from NanoSIMS. Astrobiology 10 (4), 413–424.

Pils, J.R., Laird, D.A., 2007. Sorption of tetracycline and chlortetracycline on K-and Ca-saturated soil clays, humic substances, and clay-humic complexes. Environmental science & technology 41 (6), 1928–1933.

Qin, X., Du, P., Chen, J., Liu, F., Wang, G., Weng, L., 2018. Effects of natural organic matter with different properties on levofloxacin adsorption to goethite: experiments and modeling. Chem. Eng. J. 345, 425–431.

Remusat, L., Hatton, P.-J., Nico, P.S., Zeller, B., Kleber, M., Derrien, D., 2012. NanoSIMS study of organic matter associated with soil aggregates: advantages, limitations,

and combination with STXM. Environmental Science & Technology 46 (7), 3943–3949.
Rodriguez-Mozaz, S., Chamorro, S., Marti, E., Huerta, B., Gros, M., Sànchez-Melsió, A., Borrego, C.M., Barceló, D., Balcázar, J.L., 2015. Occurrence of antibiotics and antibiotic resistance genes in hospital and urban wastewaters and their impact on the receiving river. Water Res. 69, 234–242.
Sarmah, A.K., Meyer, M.T., Boxall, A.B.A., 2006. A global perspective on the use, sales, exposure pathways, occurrence, fate and effects of veterinary antibiotics (VAs) in the environment. Chemosphere 65 (5), 725–759.
Sassman, S.A., Lee, L.S., 2005. Sorption of three tetracyclines by several soils: assessing the role of pH and cation exchange. Environmental Science & Technology 39 (19), 7452–7459.
Sedghi, S., Madani, S.H., Hu, C., Silvestre-Albero, A., Skinner, W., Kwong, P., Pendleton, P., Smernik, R.J., Rodríguez-Reinoso, F., Biggs, M.J., 2015. Control of the spatial homogeneity of pore surface chemistry in particulate activated carbon. Carbon 95, 144–149.
Sithole, B., Guy, R., 1987. Models for tetracycline in aquatic environments. Water Air Soil Pollut. 32 (3–4), 303–314.
Six, J., Elliott, E., Paustian, K., Doran, J., 1998. Aggregation and soil organic matter accumulation in cultivated and native grassland soils. Soil Sci. Soc. Am. J. 62 (5), 1367–1377.
Six, J., Elliott, E.T., Paustian, K., 1999. Aggregate and soil organic matter dynamics under conventional and no-tillage systems. Soil Sci. Soc. Am. J. 63 (5), 1350–1358.
Six, J., Conant, R., Paul, E.A., Paustian, K., 2002. Stabilization mechanisms of soil organic matter: implications for C-saturation of soils. Plant Soil 241 (2), 155–176.
Smernik, R.J., Kookana, R.S., 2015. The effects of organic matter–mineral interactions and organic matter chemistry on diuron sorption across a diverse range of soils. Chemosphere 119, 99–104.
Suan, D.T., Dmitrenko, L., 1994. Sorption kinetics of the antibiotic oxytetracycline on ion exchange materials. Appl. Biochem. Microbiol. 30 (6), 634–636.
Sutton, R., Sposito, G., 2005. Molecular structure in soil humic substances: the new view. Environmental Science & Technology 39 (23), 9009–9015.
Tfaily, M.M., Cooper, W.T., Kostka, J.E., Chanton, P.R., Schadt, C.W., Hanson, P.J., Iversen, C.M., Chanton, J.P., 2014. Organic matter transformation in the peat column at Marcell Experimental Forest: humification and vertical stratification. J Geophys Res-Biogeo 119 (4), 661–675.
Thiele-Bruhn, S., 2003. Pharmaceutical antibiotic compounds in soils—a review. J. Plant Nutr. Soil Sci. 166 (2), 145–167.
Tolls, J., 2001. Sorption of veterinary pharmaceuticals in soils: a review. Environmental Science & Technology 35 (17), 3397–3406.
Van Erp, T.S., Martens, J.A., 2011. A standardization for BET fitting of adsorption isotherms. Microporous Mesoporous Mater. 145 (1–3), 188–193.
Vogel, C., Mueller, C.W., Höschen, C., Buegger, F., Heister, K., Schulz, S., Schloter, M., Kögel-Knabner, I., 2014. Submicron structures provide preferential spots for carbon and nitrogen sequestration in soils. Nat. Commun. 5.
Wang, S., Wang, H., 2015. Adsorption behavior of antibiotic in soil environment: a critical review. Frontiers of Environmental Science & Engineering 9 (4), 565–574.
Wang, K., Xing, B., 2005. Structural and sorption characteristics of adsorbed humic acid on clay minerals. J. Environ. Qual. 34 (1), 342–349.
Wang, Z., Jiang, Q., Wang, R., Yuan, X., Yang, S., Wang, W., Zhao, Y., 2018. Effects of dissolved organic matter on sorption of oxytetracycline to sediments. Geofluids 2018, 12.
Watling, L., 1988. Small-scale features of marine-sediment and their importance to the study of deposit-feeding. Mar. Ecol. Prog. Ser. 47 (2), 135–144.
Weber, W.J., Young, T.M., 1997. A distributed reactivity model for sorption by soils and sediments. 6. Mechanistic implications of desorption under supercritical fluid conditions. Environmental Science & Technology 31 (6), 1686–1691.
Xu, X., Li, X., 2010. Sorption and desorption of antibiotic tetracycline on marine sediments. Chemosphere 78 (4), 430–436.
Zhang, H.B., Luo, Y.M., Wu, L.H., Huang, Y.J., Christie, P., 2015a. Residues and potential ecological risks of veterinary antibiotics in manures and composts associated with protected vegetable farming. Environ. Sci. Pollut. Res. 22 (8), 5908–5918.
Zhang, H., Wang, J., Zhou, B., Zhou, Y., Dai, Z., Zhou, Q., Chriestie, P., Luo, Y., 2018. Enhanced adsorption of oxytetracycline to weathered microplastic polystyrene: kinetics, isotherms and influencing factors. Environ. Pollut. 243, 1550–1557.
Zhang, Q.Q., Ying, G.G., Pan, C.G., Liu, Y.S., Zhao, J.L., 2015b. A comprehensive evaluation of antibiotics emission and fate in the river basins of China: source analysis, multimedia modelling, and linkage to bacterial resistance. Environmental science & technology 49 (11), 6772–6782.
Zhao, Y., Gu, X., Gao, S., Geng, J., Wang, X., 2012. Adsorption of tetracycline (TC) onto montmorillonite: Cations and humic acid effects. Geoderma 183–184, 12–18.
Zhou, F., 1983. Automorphous calcite crystal in seawater of the northeastern East China Sea. Proceedings of International Symposium on Sedimentation on the Continental Shelf, with Special Reference to the East China Sea, pp. 447–461.